

Article

Theoretical Investigation of the NO₃ Radical Addition to Double Bonds of Limonene

Lei Jiang ^{1,2}, Wei Wang ^{2,*} and Yi-Sheng Xu ²

¹ College of Water Sciences, Beijing Normal University, Beijing 100875, China

² Atmospheric Chemistry and Aerosol Research Division, Chinese Research Academy of Environmental Science, Beijing 100012, China; E-Mails: jiangle3657@sina.com (L.J.); xuys@craes.org.cn (Y.-S.X.)

* Author to whom correspondence should be addressed; E-Mail: wangwei@craes.org.cn (W.W.); Tel. +86-10-84915249; Fax: +86-10-84915248.

Received: 7 August 2009; in revised form: 18 August 2009 / Accepted: 19 August 2009 /

Published: 27 August 2009

Abstract: The addition reactions of NO₃ to limonene have been investigated using *ab initio* methods. Six different possibilities for NO₃ addition to the double bonds, which correspond to the two C–C double bonds (endocyclic or exocyclic) have been considered. The negative activation energies for the addition of NO₃ to limonene are calculated and the energies of NO₃-limonene radical adducts are found to be 14.55 to 20.17 kcal mol⁻¹ more stable than the separated NO₃ and limonene at the CCSD(T)/6-31G(d) + CF level. The results also indicate that the endocyclic addition reaction is more energetically favorable than the exocyclic one.

Keywords: limonene; nitrate radical (NO₃); *ab initio*; volatile organic compounds

1. Introduction

Total emissions of volatile organic compounds (VOCs) from vegetation have been estimated to be about 1,150 Tg carbon year⁻¹ [1]. More than half (54%) of the emissions are related to isoprene and monoterpenes (~11%), such as α - and β -pinene and limonene [2]. Atmospheric oxidation of VOCs, which is initiated by reactions with a variety of oxidants including OH radical, NO₃ radical and ozone is a common atmospheric chemistry reaction of the lower troposphere layer. During the day the major

sinks for VOCs are their reactions with OH radical and O₃, while with nitrate radical (NO₃) can be a very important, and often dominant, loss process at nighttime [3-6]. The reactions of NO₃ species, formed by the reaction of NO₂ and O₃ [7], with atmospheric VOCs can lead to formation of HNO₃ [8], peroxyacyl nitrate (PAN) [9], RO₂ [9,10], and toxic compounds such as dinitrates [10].

Limonene or 4-isopropenyl-1-methyl-cyclohexene is the most abundant monoterpene, and has both highly active endocyclic and exocyclic double bonds [11]. Plants non-native to Europe, e.g., Australian eucalyptus, have limonene emissions of more than 30% of monoterpene [12] and limonene represents one of the four highest terpenes emitted in North America. Many reactions of monoterpenes with OH radical and O₃ have received considerable attention with regard to their initiated oxidations, reaction kinetics, reaction products and secondary organic aerosol (SOA) formation whereas those with NO₃ have received relatively little consideration, especially the reaction of limonene with NO₃. The initial reaction of limonene and NO₃ proceeds mainly by NO₃ addition to the C–C double bond, forming the NO₃-limonene radical adduct. Under atmospheric conditions, the NO₃-limonene radical adduct is expected to react primarily with oxygen molecules to form the nitrooxyalkyl peroxy radicals, which further react with NO, engage in a self-reaction or crossreaction with other peroxy radicals, or react with HO₂. The products and aerosol formation from the NO₃ radical initiated oxidation of limonene have been investigated in the EUPHORE photoreactor facility [13]. In EUPHORE study, the results indicated that endolim had been identified as the major reaction products of the NO₃ radical initiated oxidation of limonene and the total SOA mass formed occurs mainly through the secondary chemistry of its major product endolim. Hence, the nighttime reaction between limonene and NO₃ contributes significantly to the degradation of limonene and SOA formed. However, such important processes and quantities as the formation of the NO₃-limonene radical adduct and the isomer-specific reactions have yet to be clarified.

To examine the reaction mechanism of NO₃ with limonene, a theoretical exploration of the NO₃-initiated limonene oxidation mechanism with different possibilities for the initial step of the NO₃ addition to the limonene was carried out and is reported here, as the isomeric branching of the initial NO₃ addition to limonene is crucial in determining the final product distribution. The present study is mainly focused on comparison of different reaction pathways and determination energetically favorable bonds needed for the further elaboration of the oxidation mechanisms and assessment of the products identified in experiments. Moreover, the quantum chemical study can supply some insight on the reactions between NO₃ and monoterpenes, especially important to understand the night-time atmospheric chemistry in the troposphere.

2. Theoretical Methods

The theoretical computations have been carried out on the SGI ALTIX 4700 supercomputer using the GAUSSIAN 03 suite of programs [14]. The geometry optimization of all reactants, transition states, and radical adducts was performed at UB3LYP/6-31G(d,p) with harmonic vibrational frequencies analyses. The stationary points were classified as minima in the case, when no imaginary frequencies were found, and as a transition state if only one imaginary frequency was obtained. The DFT optimized structures were then used in the single-point energy *ab initio* calculations using frozen core second-order Møller-Plesset perturbation theory (MP2) and coupled-cluster theory with single

and double excitations including perturbative corrections for the triple excitations (CCSD(T) with various basis sets to obtain accurate energy information.

Density functional theory (DFT) has been widely employed for atmospheric oxidation reactions of VOCs with NO₃ radical, OH radical and ozone [15-21]. These studies implied that deviations of the B3LYP geometries from the CASSCF ones are small enough to consider that the former level is a good compromise between quality and computational cost in the nitrate radical addition reaction and provides reasonable reaction energies and barriers for most of the ozonolysis steps insofar as the calculated B3LYP values are more accurate than those obtained with MP2 theory. So, to some degree, DFT was identified a reliable and economical method that provides a reasonable description of the VOCs-radical reactions.

In addition, for more accurate single-point energy, the basis set effects on calculated energies for NO₃-limonene reactions were corrected at MP2 level according to the recently developed method by Zhang *et al.* in his investigation of the complex reaction mechanisms and pathways of various volatile organic compounds (VOCs) in the atmosphere [22]. A correction factor (CF) was determined from the energy difference between the MP2/6-31G(d) and MP2/6-311++G(d,p) levels. The values of calculated energies were then evaluated by CCSD(T)/6-31G(d) + CF method. The applied method has been validated for several isoprene reactions initiated by NO₃, OH and O₃ [16,22,23], and of limonene initiated by O₃ [24].

3. Results and Discussion

The computational results show that there are six possibilities for the NO₃ upon addition to the double bond of the limonene, namely, four possibilities involving the endocyclic C–C double bond (see Figure 1) and two possibilities for the exocyclic C–C double bond (see Figure 2). Transition states are not found in the evaluated pathways of the NO₃ addition to limonene, which proceed in the direction of the terminal carbon atom (C9) of the exocyclic C–C double bond. This can be explained by the stronger selectivity of the NO₃ and the initial step proceeds predominantly via electrophilic addition mechanism for the reactions of NO₃ with alkenes [13,25,26].

3.1. Reaction Mechanism

T_1 diagnostic values, spin eigenvalues of the unrestricted wavefunction ($\langle S^2 \rangle$) and its projection ($\langle S^2 \rangle_A$) for all stationary points in the NO₃ addition to the limonene are provided in Table 1. All calculations of T_1 diagnostic values were run at CCSD(T)/6-31G(d)//UB3LYP/6-31G(d,p) level of theory. T_1 diagnostic values give a qualitative assessment of the nondynamical correlation significance and ensure the reliability of this treatment. For closed-shell systems, T_1 values should be under 0.02 and for open-shell systems under 0.045 [27,28].

Table 1. T_1 diagnostic values, spin eigenvalues of the unrestricted wavefunction and its projection for all stationary points in the NO_3 addition to the limonene.^a

Species	CCSD(T)/6-31G(d)	UB3LYP/6-31G(d,p)	UB3LYP/6-31G(d,p)
	T_1	$\langle S^2 \rangle$	$\langle S^2 \rangle_A$
limonene	0.0100	0.000	0.000
NO_3	0.0228	0.755	0.750
TS1	0.0211	0.761	0.750
Adduct 1	0.0148	0.754	0.750
TS2	0.0289	0.760	0.750
Adduct 2	0.0149	0.754	0.750
TS3	0.0230	0.764	0.750
Adduct 3	0.0149	0.754	0.750
TS4	0.0202	0.764	0.750
Adduct 4	0.0156	0.754	0.750
TS5	0.0220	0.768	0.750
Adduct 5	0.0146	0.754	0.750
TS6	0.0215	0.768	0.750
Adduct 6	0.0145	0.754	0.750

^aAll optimized geometries calculated at the UB3LYP/6-31G(d,p) level.

As seen from Table 1, the closed-shell T_1 diagnostic value is 0.0100 for limonene, and the the largest open-shell T_1 diagnostic value is 0.0289 for TS2. Hence, T_1 values calculated for all the stationary points are clearly under these thresholds. At the UB3LYP/6-31G(d,p) level of theory, the calculated spin eigenvalues, $\langle S^2 \rangle$, are 0.754 and 0.768 for radicals NO_3 , TS1-TS6 and Adduct1-Adduct6, respectively. After proper projection, the spin eigenvalues are reduced to 0.750 for all the open-shell stationary points, indicating that contamination of the unrestricted Hartree-Fock wave function from higher spin states is negligible.

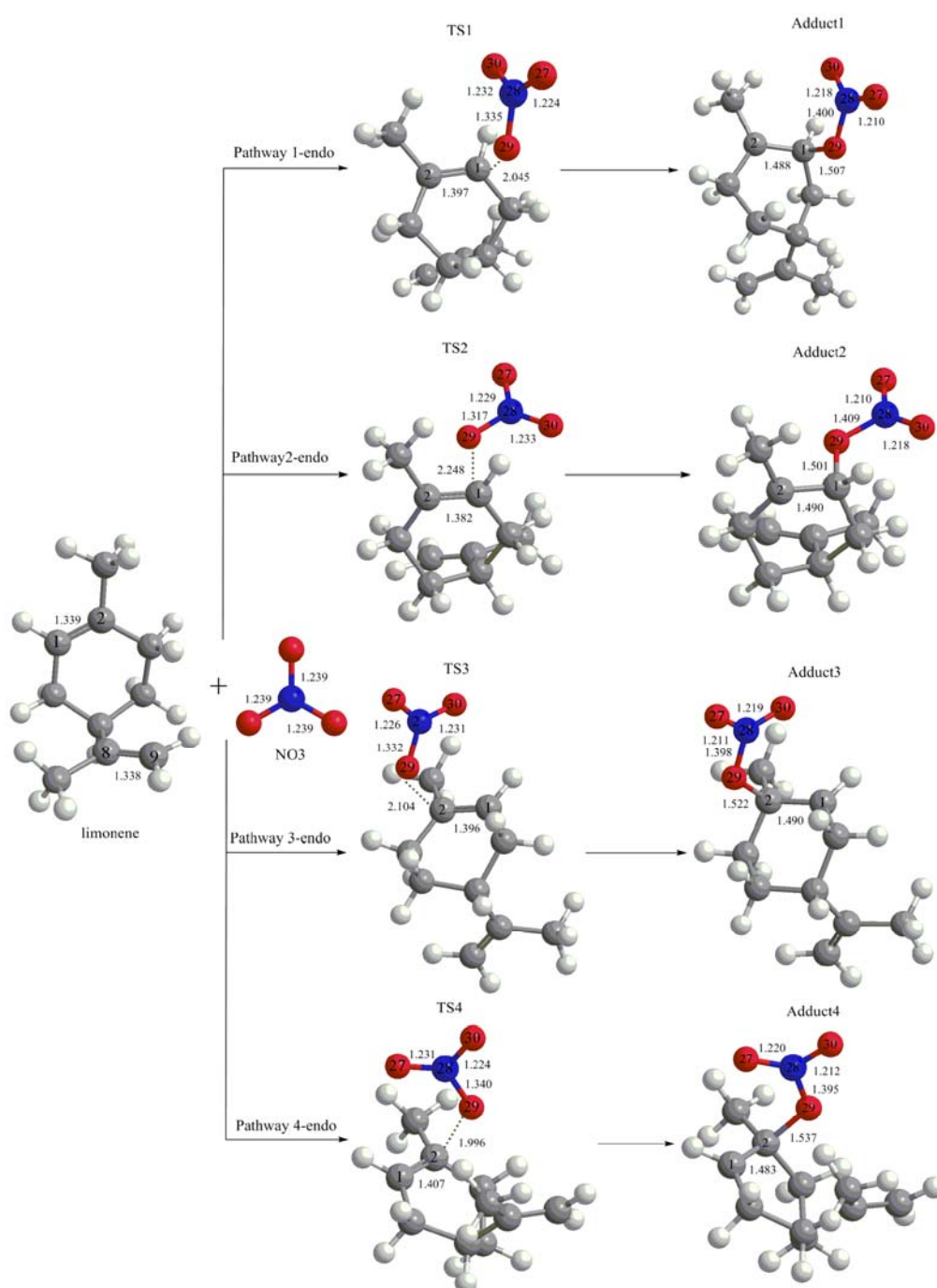
Figure 1 presents the optimized geometries of the stationary points for the NO_3 addition to the endocyclic C–C double bond obtained at the UB3LYP/6-31G(d,p) level of theory and values of the most important geometrical properties.

As seen from this Figure, the NO_3 addition reaction can proceed either on the H-substituted carbon atom (C1), or on the methyl-substituted carbon atom (C2). On each carbon atom of relevant double bond, there are two possible attacking directions. Four transition states (TS1, TS2, TS3 and TS4) associated with the addition of NO_3 to the endocyclic C–C double bond leading to the formation of the NO_3 -limonene radical adducts (Adduct1-Adduct4) have been identified. Each transition state has only one imaginary harmonic vibrational frequency and can be classified as the first-order saddle point. The values of imaginary frequencies for TS1, TS2, TS3, and TS4 transition states are 157.10i, 67.07i, 157.82i, and 228.95i, respectively.

In the 1-endo pathway, the C–C double bond distance (1.339 Å), increases by 0.058 Å and 0.149 Å in the transition states (TS1) and NO_3 -limonene radical adduct (Adduct1), respectively, which clearly demonstrates that a single bond property on the formation of the NO_3 -limonene radical adducts presented during the reaction procedure. The disappearance of the double bond is also shown in the reaction channel. The NO_3 -limonene distance in the TS1 is 2.045 Å, while in the Adduct1 is 1.507 Å.

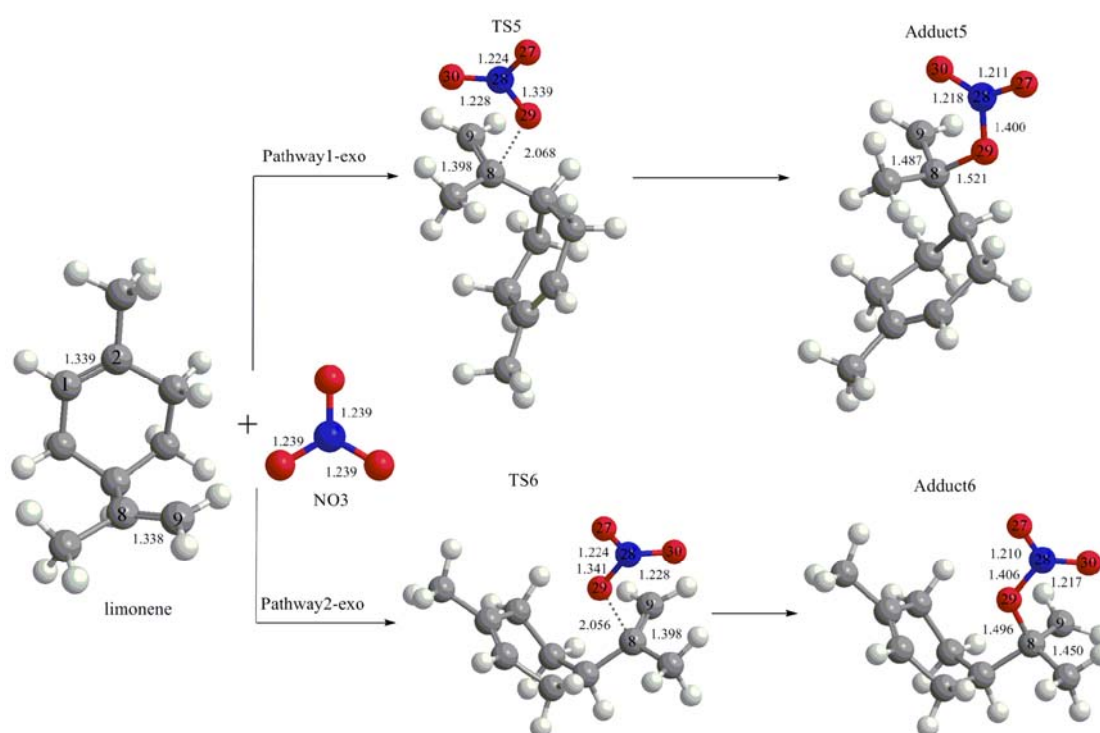
In NO_3 radical, the three N–O bond lengths are the same values (1.239 Å). While in the TS1, the length of the N–O bond oriented towards the C–C double bond, increases a length of 0.096 Å and becomes to 1.400 Å for the Adduct1. Meanwhile it shows decreasing tendency to the other two bonds. Compared with those in the NO_3 radical, the bond lengths have less variation and decrease 0.007–0.029 Å in the TS1 and Adduct1. Other three pathways of transition states (TS2, TS3 and TS4) and NO_3 -limonene radical adducts (Adduct2, Adduct 3 and Adduct 4) exhibit a similar pattern.

Figure 1. Geometries of stationary points involved in the NO_3 addition to limonene endocyclic double bond obtained at UB3LYP/6-31G(d,p) level of theory. Bond distances are given in Å. TS1, TS2, TS3, and TS4 are abbreviations for 1-endo, 2-endo, 3-endo and 4-endo transition states, respectively.



The optimized geometries for the NO₃ addition to the exocyclic C–C double bond are illustrated in Figure 2. In this case, the NO₃ addition could proceed on the methyl-substituted carbon atom (C8). Two transition states (TS5 and TS6) associated with the addition of NO₃ to the exocyclic C–C double bond leading to the formation of the NO₃-limonene radical adducts (Adduct5 and Adduct6) have been identified too. The values of imaginary frequencies for TS5 and TS6 transition states are 191.62i and 231.50i, respectively.

Figure 2. Geometries of stationary points involved in the NO₃ addition to limonene exocyclic double bond obtained at UB3LYP/6-31G(d,p) level of theory. Bond distances are given in Å. TS5 and TS6 are abbreviations for 1-exo and 2-exo transition states, respectively.



In comparison of the 1-endo pathway, the 1-exo and 2-exo pathways exhibited a similar addition mode are shown in Figure 2. The C–C double bond distance (1.338 Å), increases by a length of 0.06 Å in the transition states (TS), and to 1.450–1.487 Å in the NO₃-limonene radical adducts, and clearly becomes a single bond. The NO₃-limonene radical distance in the two TS is in the range of 2.056–2.068 Å, and in the two adduct isomers is between 1.496 and 1.521 Å. In the TS, the length of the N–O bond oriented towards the C–C double bond, increases lengths in the range of 0.1–0.102 Å and increases to 1.400–1.406 Å in the adduct isomers. While the other two N–O bonds lengths vary less and decrease 0.011–0.029 Å in the TS and adduct isomers.

3.2. Thermochemical Analysis

The NO₃-limonene reaction energies computed at different levels of theory with different basis sets with the zero-point correction included are presented in Table 2. As seen from this data, the reaction

energies of the NO₃ addition to limonene calculated at different levels of theory are quite different. The values predicted by MP2/6-31G(d) and B3LYP/6-311 + G(3df,2pd) are comparable and differ by -2.7–2.28 kcal mol⁻¹. The values obtained at CCSD(T)/6-31G(d) level theory are 5.32–13.52 kcal mol⁻¹ more stable than those calculated with MP2 and B3LYP. Another important detail is that the values determined by using MP2 and B3LYP and with two different basis sets differ by 1.71–2.73 kcal mol⁻¹ and 3.22–4.06 kcal mol⁻¹, respectively. At the CCSD(T)/6-31G(d) + CF level of theory, the NO₃-limonene radical adducts are 14.55–20.17 kcal mol⁻¹ more stable than the separate NO₃ and limonene. Adduct2 is more stable than others, The difference in the relative stability of the six NO₃-limonene radical adducts does not exceed 5.62 kcal mol⁻¹.

Table 2. NO₃-limonene Reaction Energies (RE) with Zero-Point Correction Included (kcal mol⁻¹) computed at different levels of theory for the six pathways ^a.

Method	RE _{1-endo}	RE _{2-endo}	RE _{3-endo}	RE _{4-endo}	RE _{1-exo}	RE _{2-exo}
PMP2/6-31G(d)	-9.76	-12.19	-11.41	-5.68	-9.15	-8.72
PMP2/6-311++G(d,p)	-7.06	-9.46	-8.99	-3.97	-6.45	-6.18
B3LYP/6-31G(d,p)	-15.26	-16.90	-14.00	-8.73	-11.26	-10.08
B3LYP/6-311 + G(3df,2pd)	-12.04	-13.15	-10.43	-4.91	-7.25	-6.02
CCSD(T)/6-31G(d)	-20.58	-22.90	-21.90	-16.26	-19.12	-18.55
CCSD(T)/6-31G(d) + CF	-17.88	-20.17	-19.49	-14.55	-16.42	-16.02

^a optimized geometries, vibrational frequencies and ZPE obtained at the UB3LYP/6-31G(d,p) level.

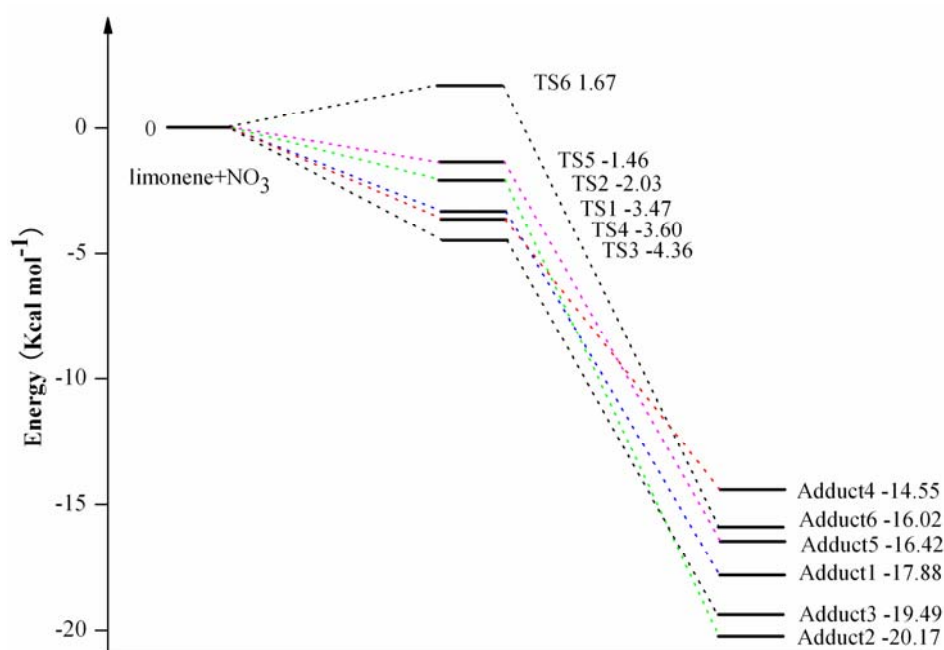
The NO₃-limonene activation energies with the zero-point correction (ZPE) included computed at different levels of theory with different basis sets, are given in Table 3. As seen from this Table, the activation energies for the formation of the NO₃-limonene reactions with the zero-point correction included are very sensitive to the effects of electron correlation and basis set. The activation energies of the NO₃-limonene reaction are positive activation energies and significantly overestimate with MP2 method. B3LYP/6-311 + G(d,p), B3LYP/6-311 + G(3df,2pd) (except for ΔE_{2-exo}), CCSD(T)/6-31G(d) and CCSD(T)/6-31G(d) + CF (except for ΔE_{2-exo}) levels are negative activation energies, which corresponds to the NO₃ + propene reaction, ozonolysis of isoprene and the OH + ethane reaction reported in the previous theoretical studies [15,22,29,30]. The negative activation energies given by B3LYP/6-311 + G(3df,2pd) and CCSD(T)/6-31G(d) are comparable, with a largest difference of 4.04 kcal mol⁻¹ for ΔE_{2-exo} . Compared with CCSD(T)/6-31G(d) + CF, there are noticeable differences in the calculated activation energies for the NO₃-limonene reaction with the UB3LYP/6-31G(d,p) methods of and results differ by 1.12–5.98 kcal mol⁻¹, while there are little differences with B3LYP/6-311 + G(3df,2pd), and they differ by -0.6–3.32 kcal mol⁻¹. The activation energies obtained at the CCSD(T)/6-31G(d) + CF level of theory are -3.47 kcal mol⁻¹ for 1-endo, -2.03 kcal mol⁻¹ for 2-endo, -4.36 kcal mol⁻¹ for 3-endo, -3.60 kcal mol⁻¹ for 4-endo, -1.43 kcal mol⁻¹ for 1-exo and 1.67 kcal mol⁻¹ for 2-exo. This indicates that 3-endo is the most favorable pathway. It also implies that the endocyclic addition is more energetically favorable than the exocyclic one and that the NO₃ attack predominantly takes place at the endo-double bonded carbons.

Table 3. NO₃-limonene Activation Energies (ΔE) with Zero-Point Correction Included (kcal mol⁻¹) computed at different levels of theory for the six pathways ^a.

Method	ΔE_{1-endo}	ΔE_{2-endo}	ΔE_{3-endo}	ΔE_{4-endo}	ΔE_{1-exo}	ΔE_{2-exo}
PMP2/6-31G(d)	7.20	13.68	7.68	7.15	8.62	11.06
PMP2/6-311++G(d,p)	10.06	16.06	10.55	9.41	11.94	14.50
B3LYP/6-31G(d,p)	-8.17	-8.01	-7.72	-4.72	-4.34	-0.92
B3LYP/6-311 + G(3df,2pd)	-6.47	-5.35	-5.46	-2.02	-1.30	2.27
CCSD(T)/6-31G(d)	-6.34	-4.41	-7.23	-5.86	-4.78	-1.77
CCSD(T)/6-31G(d) + CF	-3.47	-2.03	-4.36	-3.60	-1.46	1.67

^a optimized geometries, vibrational frequencies and ZPE obtained at the UB3LYP/6-31G(d,p) level.

As seen from Table 3, relatively low activation or slightly negative energies obtained for the reaction of NO₃ with limonene in our work, which agree with the values obtained for the reaction of NO₃ with alkenes and other terpenes. Hence, the reaction of the NO₃ addition to limonene is entirely consistent with a radical addition process [25]. Figure 3 illustrates the relative energies of the stationary points located on the singlet ground-state separate NO₃ and limonene potential energy surface at the CCSD(T)/6-31G(d) + CF level of theory.

Figure 3. NO₃-limonene reaction coordinates: relative energies of the stationary points located on the separate NO₃ and limonene ground-state potential energy surface. The energy values are given in kcal mol⁻¹ and are calculated using CCSD(T)/6-31G(d) + CF//UB3LYP/6-31G(d,p).

The NO₃-limonene reaction enthalpies, Gibbs free energies and entropies computed at B3LYP/6-31G(d,p) level of theory with the thermal Correction included, are shown in Table 4. The NO₃-limonene addition reaction is exothermic for the six pathways. The six radical adducts (Adduct1-Adduct6) are 9.32–17.42 kcal mol⁻¹ more stable than the reactants. The endocyclic addition

reactions are more stabilized than the exocyclic addition reaction, except for the 4-endo pathway. In the endocyclic addition reactions, the Adduct2, corresponding to the 2-endo pathway, is the most stabilized, with value of $-17.42 \text{ kcal mol}^{-1}$. Adduct5 is more stabilized, with a value of $-11.73 \text{ kcal mol}^{-1}$, corresponding to the 1-exo pathway in the exocyclic addition reactions. The NO_3 -limonene reaction Gibbs free energies range from -4.69 to $3.61 \text{ kcal mol}^{-1}$ for the six pathways. The values of Gibbs free energies are negative for 1-endo, 2-endo and 3-endo pathways, implying that the reaction of NO_3 with limonene can take place spontaneously.

Additionally, the formation of a prereactive van der Waals complex has been used to explain the negative values found for the experimental activation energies [31]. A van der Waals complex was formed prior to addition have been reported in quantum chemical studies on the OH addition reaction to alkenes [30,32,33]. A transition state connecting the van der Waals complex with the adduct has also been found. But, as for the case of the propene + NO_3 reaction, no van der Waals complexes in the limonene + NO_3 reaction have been found at the UB3LYP/ 6-31G(d,p) level of calculation, since the DFT method fails in case of Van der Waals and loose transition states and actually represent only small irregularities on the potential energy hypersurface [15]. The van der Waals complexes do not have a profound effect on the kinetics [30] and are not chemically relevant in the reaction mechanisms [34], although they will probably exist.

Table 4. NO_3 -limonene Reaction Enthalpies, Gibbs Free Energies and Entropies (ΔH and ΔG in kcal mol^{-1} , ΔS in $\text{cal mole}^{-1}\text{K}^{-1}$) with Thermal Correction Included computed at B3LYP/6-31G(d,p) level of theory for the six pathways ^a.

Method	1-endo	2-endo	3-endo	4-endo	1-exo	1-exo
ΔH	-15.59	-17.42	-14.70	-9.32	-11.73	-10.55
ΔG	-3.64	-4.69	-0.97	3.61	1.80	2.83
ΔS	-40.08	-42.70	-46.05	-43.37	-45.38	-44.88

^a optimized geometries, vibrational frequencies and Thermal Correction to Enthalpy and Gibbs Free Energy obtained at the UB3LYP/6-31G(d,p) level.

4. Conclusions

Our theoretical investigation reveals several important aspects regarding the gas phase reaction of the initial NO_3 addition to the limonene using computational quantum, which has importance in night-time atmospheric chemistry.

(1) The activation energies for the formation of the NO_3 -limonene reaction have been determined first. At CCSD(T)/6-31G(d) + CF//UB3LYP/6-311 + G(d,p), our results indicate that relatively low activation or slightly negative energies were obtained, and 3-endo pathway is the most favorable branching for the initial step of the NO_3 -limonene reactions. From the obtained activation energies, we concluded that the reaction of the NO_3 addition to limonene is entirely consistent with a radical addition process.

(2) The calculated activation energies of the NO_3 -limonene reactions are very sensitive to electron correlation and basis set effects. The activation energies of the NO_3 -limonene reaction were significantly overestimated with the MP2 method. Compared with CCSD(T)/6-31G(d) + CF, there are

noticeable differences in the calculated activation energies for the NO₃-limonene reaction with the methods of UB3LYP/6-31G(d,p), while there was little difference with B3LYP/6-311 + G(3df,2pd).

(3) Six possibilities for the NO₃ addition to double bond on the limonene were found; the two possibilities for the NO₃ addition proceeding on the terminal carbon atom (C9) of the exocyclic C–C double bond are not found. The endocyclic addition is more energetically favorable than the exocyclic one. Those are consistent with the EUPHORE study by Spittler *et al.*, who could not detect the products formaldehyde or 4-acetyl-1-methylcyclohex-1-ene, an indication of an attack of NO₃ on the exocyclic double bond in limonene. Hence, the computation results verified that the high selectivity of NO₃ towards different C–C double bonds and the initial step proceeds predominantly via electrophilic addition for the reactions of NO₃ with limonene.

Acknowledgements

This work was supported by National Natural Science Foundation of China (Grant 40705043), Social Public Welfare Projects (Grant no. 200809152) and the Science Foundation of Chinese Research Academy of Environmental Science (Grant 2007KYYW36). Additional support was provided by the CRAES Supercomputing Facilities (SGI 4700 supercomputers).

References

1. Gill, K.J.; Hites, R.A. Rate constants for the gas-phase reactions of the hydroxyl radical with isoprene, α - and β -pinene, and limonene as a function of temperature. *J. Phys. Chem. A* **2002**, *106*, 2538-2544.
2. Guenther, A.; Hewitt, C.N.; Erickson, D.; Fall, R.; Geron, C.; Graedel, T.; Harley, P.; Klinger, L.; Lerdau, M.; McKay, W.A.; Pierce, T.; Scholes, B.; Steinbrecher, R.; Tallamraju, R.; Taylor, J.; Zimmerman, P.J. A global model of natural volatile organic compound emissions. *J. Geophys. Res.* **1995**, *100*, 8873-8892.
3. Grosjean, D.; Williams, E.L.; Grosjean, E.; Andino, J.M.; Seinfeld, J.H. Atmospheric oxidation of biogenic hydrocarbons, reactions of ozone with β -pinene, d-limonene and transcarophyllene. *Environ. Sci. Technol.* **1993**, *27*, 2754-2758.
4. Kleindienst, T.E.; Harris, G.H.; Pitts, J.N., Jr. Rates and temperature dependence of the reaction of OH with isoprene, its oxidation products, and selected terpenes. *Environ. Sci. Technol.* **1982**, *16*, 844-846.
5. Shu, Y.; Atkinson, R. Rate constants for the gas-phase reactions of O₃ with a series of terpenes and OH radical formation from the O₃ reactions with sesquiterpenes at 296 \pm 2 K. *Int. J. Chem. Kinet.* **1994**, *26*, 1193-1205.
6. Atkinson, R. Gas-phase tropospheric chemistry of organic compounds. *J. Phys. Chem. Ref. Data, Monogr.* **1994**, *2*, 1-216.
7. Wayne, R.P. The nitrate radical: Physics, chemistry and the atmosphere. *Atmos. Environ.* **1991**, *25A*, 1-206.

8. Atkinson, R.; Plum, C.N.; Carter, W.P.L.; Winer, A.M.; Pitts, J.N., Jr. Kinetics of the gas-phase reactions of NO₃ radicals with a series of alkanes at 296 ± 2K. *J. Phys. Chem.* **1984**, *88*, 2361-2364.
9. Cantrell, C.A.; Davidson, J.A.; Busarow, K.L.; Calvert, J.G. The CH₃CHO-NO₃ reaction and possible night-time PAN generation. *J. Geophys. Res.* **1986**, *91*, 5347-5353.
10. Bandow, H.; Okuda, M.; Akimoto, H. Mechanism of the gas-phase reactions of propylene and nitroxy radicals. *J. Phys. Chem.* **1980**, *84*, 3604-3608.
11. Guenther, A.; Geron, C.; Pierce, T.; Lamb, B.; Harley, P.; Fall, R. Natural emissions of non-methane volatile organic compounds, carbon monoxide, and oxides of nitrogen from North America. *Atmos. Environ.* **2000**, *34*, 2205-2230.
12. He, C.; Murray, F.; Lyons, T. Monoterpene and isoprene emissions from 15 eucalyptus species in Australia. *Atmos. Environ.* **2000**, *34*, 645-655.
13. Spittler, M.; Barnes, I.; Bejan, I.; Brockmann, K.J.; Benter, Th.; Wirtz, K. Reactions of NO₃ radicals with limonene and α -pinene: Product and SOA formation. *Atmos. Environ.* **2006**, *40*, S116-S127.
14. Frisch, M.J.; Trucks, G.W.; Schlegel, H.B.; Scuseria, G.E.; Robb, M.A.; Cheeseman, J.R.; Montgomery, J.A., Jr.; Vreven, T.; Kudin, K.N.; Burant, J.C.; Millam, J.M.; Iyengar, S.S.; Tomasi, J.; Barone, V.; Mennucci, B.; Cossi, M.; Scalmani, G.; Rega, N.; Petersson, G.A.; Nakatsuji, H.; Hada, M.; Ehara, M.; Toyota, K.; Fukuda, R.; Hasegawa, J.; Ishida, M.; Nakajima, T.; Honda, Y.; Kitao, O.; Nakai, H.; Klene, M.; Li, X.; Knox, J.E.; Hratchian, H.P.; Cross, J.B.; Bakken, V.; Adamo, C.; Jaramillo, J.; Gomperts, R.; Stratmann, R.E.; Yazyev, O.; Austin, A.J.; Cammi, R.; Pomelli, C.; Ochterski, J.W.; Ayala, P.Y.; Morokuma, K.; Voth, G.A.; Salvador, P.; Dannenberg, J.J.; Zakrzewski, V.G.; Dapprich, S.; Daniels, A.D.; Strain, M.C.; Farkas, O.; Malick, D.K.; Rabuck, A.D.; Raghavachari, K.; Foresman, J.B.; Ortiz, J.V.; Cui, Q.; Baboul, A.G.; Clifford, S.; Cioslowski, J.; Stefanov, B.B.; Liu, G.; Liashenko, A.; Piskorz, P.; Komaromi, I.; Martin, R.L.; Fox, D.J.; Keith, T.; Al-Laham, M.A.; Peng, C.Y.; Nanayakkara, A.; Challacombe, M.; Gill, P.M.W.; Johnson, B.; Chen, W.; Wong, M.W.; Gonzalez, C.; Pople, J.A. *Gaussian 03*, Revision E.01; Gaussian, Inc.: Wallingford, CT, USA, 2004.
15. Pérez-Casany, M.P.; Nebot-Gil, I.; Sánchez-Marín, J. *Ab initio* study on the mechanism of tropospheric reactions of the nitrate radical with alkenes: Propene. *J. Phys. Chem. A*, **2000**, *104*, 6277-6286.
16. Suh, I.; Lei, W.; Zhang, R. Experimental and theoretical studies of isoprene reaction with NO₃. *J. Phys. Chem. A* **2001**, *105*, 6471-6478.
17. Lei, W.; Zhang, R.; McGivern, W.S.; Derecskei-Kovacs, A.; North, S.W. Theoretical study of isomeric branching in the isoprene-OH reaction: Implications to final product yields in isoprene oxidation. *Chem. Phys. Lett.* **2000**, *326*, 109-114.
18. Vereecken, L.; Peeters, J. Theoretical study of the formation of acetone in the OH-initiated atmospheric oxidation of α -pinene. *J. Phys. Chem. A* **2000**, *104*, 11140-11146.
19. Gutbrod, R.; Kraka, E.; Schindler, R.N.; Cremer, D. Kinetic and theoretical investigation of the gas-phase ozonolysis of isoprene: Carbonyl oxides as an important source for OH radicals in the atmosphere. *J. Am. Chem. Soc.* **1997**, *119*, 7330-7342.

20. Olzmann, M.; Kraka, E.; Cremer, D.; Gutbrod, R.; Andersson, S. Energetics, kinetics, and product distributions of the reactions of ozone with ethene and 2,3-dimethyl-2-butene. *J. Phys. Chem. A* **1997**, *101*, 9421-9429.
21. Aplincourt, P.; Ruiz-López, M.F. Theoretical study of formic acid anhydride formation from carbonyl oxide in the atmosphere. *J. Phys. Chem. A* **2000**, *104*, 380-388.
22. Lei, W.; Derecskei-Kovacs, A.; Zhang, R. *Ab initio* study of OH addition reaction to isoprene. *J. Chem. Phys.* **2000**, *113*, 5354-5360.
23. Zhang, D.; Zhang, R. Mechanism of OH formation from ozonolysis of isoprene: A quantum-chemical study. *J. Am. Chem. Soc.* **2002**, *124*, 2692-2703.
24. Jiang, L.; Wang, W.; Xu, Y. *Ab initio* investigation of O₃ addition to double bonds of limonene. submitted for publication.
25. Martínez, E.; Cabañas, B.; Aranda, A.; Martín, P.; Salgado, S. Absolute rate coefficients for the gas-phase reactions of NO₃ radical with a series of monoterpenes at T=298 to 433 K. *J. Atmos. Chem.* **1999**, *33*, 265-282.
26. Shu, Y.; Kwok, E.S.C.; Tuazon, E.C.; Atkinson, R.; Arey, J. Products of the gas-phase reactions of linalool with OH radicals, NO₃ radicals, and O₃. *Environ. Sci. Technol.* **1997**, *31*, 896-904.
27. Lee, T.J.; Taylor, P.R. A diagnostic for determining the quality of single-reference electron correlation methods. *Int. J. Quantum Chem. Symp.* **1989**, *23*, 199-207.
28. Rienstra-Kiracofe, J.C.; Allen, W.D.; Schaefer, H.F., III. The C₂H₅ + O₂ reaction mechanism: High-level *ab initio* characterizations. *J. Phys. Chem. A* **2000**, *104*, 9823-9840.
29. Pérez-Casany, M.P.; Nebot-Gil, I.; Sánchez-Marín, J. DFT theoretical study on the reaction mechanism of the nitrate radical with alkenes: 2-Butene, isobutene, 2-methyl-2-butene, and 2,3-dimethyl-2-butene. *J. Phys. Chem. A* **2000**, *104*, 10721-10730.
30. Alvarez-Idaboy, J.R.; Mora-Díez, N.; Vivier-Bunge, A. A quantum chemical and classical transition state theory explanation of negative activation energies in OH addition to substituted ethenes. *J. Am. Chem. Soc.* **2000**, *122*, 3715-3720.
31. Mozurkewich, M.; Lamb, J.J.; Benson, S.W. Negative activation energies and curved Arrhenius plots. 2. Hydroxyl + carbon monoxide. *J. Phys. Chem.* **1984**, *88*, 6435-6441.
32. Ramírez-Ramírez, V.M.; Nebot-Gil, I. Theoretical study of the OH addition to the endocyclic and exocyclic double bonds of the d-limonene. *Chem. Phys. Lett.* **2005**, *409*, 23-28.
33. Díaz-Acosta, I.; Alvarez-Idaboy, J.R.; Vivier-Bunge, A. Mechanism of the OH-propene-O₂ reaction: An *ab initio* study. *Int. J. Chem. Kinet.* **1999**, *31*, 29-36.
34. García-Cruz, I.; Ruiz-Santoyo, M.E.; Alvarez-Idaboy, J.R.; Vivier-Bunge, A. *Ab-initio* study of initial atmospheric oxidation reactions of C₃ and C₄ alkanes. *J. Comput. Chem.* **1999**, *20*, 845-856.